

Military Technical College,
Kobry El-Kobbah,
Cairo, Egypt



9th International Conference
On Aerospace Sciences &
Aviation Technology

ANALYSIS OF JAMMING TECHNIQUE AGAINST IAC MONOPULSE RADAR

Makaryus* A. H., El-Mahdy* A. A., El gamel* S. A.

ABSTRACT

This paper presents the mathematical analysis of a proposed jamming technique used against IAC monopulse radar. The idea of this technique is to repeat the radar signal with change in its amplitude and phase (deception jamming signal) to produce an angular error in the target tracker. This error changes for different values of amplitude ratio and phase difference w.r.t the target signal. In the generated deceptive jamming signals, the change in the amplitude ratio makes large effect than the change in the phase difference on the real part of the complex measured error angle. The real value of the complex measured angle due to jamming with constant phase difference and different amplitude ratio has large variation at amplitude ratio less than three. This value converges to the value of the angle of the false target for higher amplitude ratio. There is no jamming effect at amplitude ratios less than one and for some values of phase difference. At these values, the measured angle equals to the angle of the real target. At least two jamming signals are required to have the complex error jamming angle to overcome the ECCM techniques that might be used by the target.

KEY WORDS: Jamming, and IAC monopulse radar

* Egyptian Armed Forces

I. Introduction

Monopulse radars are commonly used in target tracking because of their angular accuracy. These radars provide a better angular accuracy and less sensitivity to fluctuation in the radar cross section (RCS) of the target compared with other types of tracking radars (such as sequential lobbing and conical scan). In practice these radars use four lobes (two for elevation angle measurements and the others for azimuth angle). The echo received by the four lobes are mixed in a hybrid junction to provide three signals, namely the summation and two difference (in azimuth and in elevation). The target angle with respect to (w.r.t) the radar axis is measured via computation of variable named monopulse ratio, which is the ratio of the two difference signals (D_x, D_y) and the sum signal S (in the phasor form) [1,2].

This paper is organized as follows. Section II represents the mathematical formulation of the proposed jammer. The Mathematical Analysis of the Proposed Jamming Technique is discussed in section III. Section IV represents the Performance of the proposed Jamming technique Under Possible ECCM Techniques. In Section V the conclusion of this paper is introduced.

II. Mathematical Formulation of the Proposed Jammer

The proposed jamming signal consists of composite CW pulsed signals with different amplitudes, phases, and delays; the generated jamming signal has the following form

$$S_j = \sum_{n=1}^N A_n \cos[\omega_c(t + \tau_n) + \varphi_n], \quad 0 < t < \delta \quad (1)$$

where S_j is the jammer transmitted signal, A_n is the amplitude of the n th CW jamming signal, ω_c is the angular carrier frequency, τ_n is the relative time delay (relative to the missile signal), and φ_n is the relative phase difference. The effect of this composite jamming signal appears as multiple false targets, each false target corresponds to one of the CW jamming signals. These false targets lie in the same range gate of the missile tracking radar. The total effect of this action is that these targets appear as one target different from the real target. The idea of the proposed jamming technique is to introduce an angular error in the target measured angle in IAC monopulse tracking radar. The mathematical formulation of the measured target angle under jamming is expressed as

$$\frac{1}{\rho} \frac{D}{S} = \theta_j = \frac{\theta_o + \theta_1 g_1 e^{j\phi_1} + \dots + \theta_N g_N e^{j\phi_N}}{1 + g_1 e^{j\phi_1} + \dots + g_N e^{j\phi_N}} \quad (2)$$

where θ_j is the new complex measured angle due to jamming. This angle results from real target (at angle θ_o) and N false unresolved targets at angles $\theta_1, \theta_2, \dots, \theta_N$.

III. Mathematical Analysis of the Proposed Jamming Technique

We start the analysis of the mathematical results given in (2) by considering $n=1$, then we can write the complex angle (θ_j) in the following form

$$\theta_j = \frac{\theta_o + \theta_1 g_1 e^{j\phi_1}}{1 + g_1 e^{j\phi_1}} \quad (3)$$

recall that θ_o is the angle of the real target and θ_1 is the angle of a false target. The angles θ_o and θ_1 must lie inside the half power beam width (HPBW) of the missile pattern. The considered value of HPBW is equal 1° . For analysis purposes, we assume some values for the angles θ_o and θ_1 that lie in HPBW. These values are 0.1° and 0.5° for θ_o and θ_1 respectively. As shown in Fig.1, the graphical representation of the measured complex angle (θ_j) for fixed value of g_1 and varying the phase difference ϕ_1 from ($0^\circ \rightarrow 360^\circ$) represents a circle in the complex plane. Varying the values of g_1 result in multiple circles. The centers of these circles always lie on the real axis. The circles for $g_1 < 1$ lie in the left hand side of the imaginary axis (the midpoint of θ_o and θ_1). As g_1 decreases, we have smaller circles that approach to θ_o . When g_1 reaches zero the resulting circle becomes a point in the real axis, which is θ_o . The circles for $g_1 > 1$ lie in the right hand side of the imaginary axis. As g_1 increases, we have smaller circles that approach to θ_1 . When g_1 is a very large value (\approx infinity), the resulting circle becomes a point in the real axis which is θ_1 . At $g_1 = 1$, the complex angle θ_j has no real value, it is represented by an imaginary line (because the imaginary axis is shifted to the midpoint of θ_o and θ_1) as shown in Fig.1.

Moreover, if the values of g_1 is varying from ($0 \rightarrow \infty$), for fixed value of the phase difference ϕ_1 , we have a group of circles that move along the imaginary axis and always pass through the two angles θ_o and θ_1 in the real axis as shown in Fig.2.

In Fig.3, the measured value of θ_j is the intersection of two circles. The first circle (bold one) has a constant g_1 (equal to 1.5) and varying ϕ_1 from ($0^\circ \rightarrow 360^\circ$), and

the second circle (thin one) has constant ϕ_1 (equal to 30°) and varying g_1 from $(0 \rightarrow \infty)$. Similar results can be obtained by increasing n in (2) as shown in Fig.4. This figure shows that for $n=2$, the value of θ_j is the intersection of four circles (two bold circles for constant g_1 and g_2 and varying ϕ_1 and ϕ_2 from $(0^\circ \rightarrow 360^\circ)$, and two thin circles for constant ϕ_1 and ϕ_2 and varying g_1 and g_2 from $(0 \rightarrow \infty)$).

Generally for $n=N$, we have $2N$ circles and the value of θ_j is the intersection of all of them.

Fixed amplitude ratio g_1 and different values of phase difference ϕ_1 result in different values of the angle θ_j (intersection in points a1, b1, c1, d1) as shown in Fig.5. Fixed phase difference ϕ_1 and different amplitude ratio g_1 results in different values for the angle θ_j (intersection in points a2, b2, c2, d2) as shown in Fig.6. From Figs 5 and 6, we can conclude that the variation of ϕ_1 at fixed g_1 provides smaller effect on the angle θ_j than varying g_1 at fixed ϕ_1 .

Another way to study (2) is to plot the amplitude ratio g_1 versus the measured angle θ_j for different phase difference. This plot is shown in Fig.7, a zoom in on this figure is shown in Fig.7a. This figure shows that the same θ_j is obtained for ϕ_1 and $(360^\circ - \phi_1)$, so it's enough to change ϕ_1 from $(0^\circ \rightarrow 180^\circ)$ to have a change in θ_j . All curves converge to $\theta_j = 0.5$ for high g_1 (they tend to reach 0.5 for $g_1 > 10$) and for small value of g_1 ($g_1 < 3$); we have high change in the angle θ_j .

The relation between the phase differences ϕ_1 versus the measured angle θ_j for different values of g_1 is shown in Fig.8. This figure shows that, for all phase difference from $(0^\circ \rightarrow 360^\circ)$ at $g_1 = 0$, the angle $\theta_j = 0.1$ (equal to θ_o). For $g_1 = 1$ the jamming angle $\theta_j = 0.3$ (midpoint between θ_o and θ_1). For very high g_1 the jamming angle $\theta_j = 0.5$ (equal to θ_1). From this figure, it's clear that all curves are mirror imaged at $\phi_1 = 180^\circ$ (so that the real of the angle θ_j for (ϕ_1) and $(360^\circ - \phi_1)$ at constant g_1 are equal). All curves for $g_1 > 1$, the real of the measured angles are above 0.3° . For $g_1 < 1$, the real of the measured angles are below 0.3° . All these curves for reciprocal values of g_1 are imaged to each other midpoint between θ_o and θ_1 .

Now, we study (2) for $n > 1$, let $n=2$ in then it can be written as follows

$$\theta_j = \frac{\theta_o + \theta_1 g_1 e^{j\phi_1} + \theta_2 g_2 e^{j\phi_2}}{1 + g_1 e^{j\phi_1} + g_2 e^{j\phi_2}} \quad (4)$$

The following discussion is made for the following parameters $\theta_o = 0.1$, $\theta_1 = 0.3$, $\theta_2 = 0.5$, $g_1 = 0.5$ and $\phi_1 = 30^\circ$. We plot the amplitude ratio g_2 versus the measured angle θ_j for different phase difference ϕ_2 . This plot is shown in Fig.9, a zoom in on this figure is shown in Fig.9a. All curves converge to $\theta_j = 0.5$ for high g_2 (they tend to reach 0.5 for $g_2 > 10$) and for small value of g_2 ($g_2 < 3$); we have high change in the angle θ_j .

The relation between the phase differences ϕ_2 versus the measured angle θ_j for different values of g_2 is shown in Fig.10. This figure differs from Fig.8, for all phase difference from ($0^\circ \rightarrow 360^\circ$) at $g_2 = 0$, the angle $\theta_j = \text{constant}$ (it is not equal to θ_o). For very high g_2 the jamming angle $\theta_j = 0.5$ (equal to θ_1). All curves for $g_1 > 1$, the real of the measured angles are above 0.3° . For $g_1 < 1$, the real of the measured angles are below 0.3° .

IV. Performance of the Jamming Under Possible ECCM Techniques

For a single target, the angle measured by the monopulse tracking radar is real. The presence of jamming signal changes the real part and produces an imaginary part, then the IAC monopulse tracking radar starts to resolve between the real and jamming signal. One of the possible ECCM techniques used against the proposed jammer is called two pulse solution [3,4]. To illustrate the idea of this techniques we consider ($n=1$) in equation (2). Then the complex angle under jamming θ_j is written in the form

$$\theta_j = \frac{\theta_o + \theta_1 g_1 e^{j\phi_1}}{1 + g_1 e^{j\phi_1}} \quad (5)$$

The complex angle (θ_j) can be written in the form $x + jy$. Separating the complex angle θ_j to a real and imaginary parts as follows,

$$x + jy = \frac{\theta_o + \theta_1 g_1 [\cos \phi_1 + j \sin \phi_1]}{1 + g_1 [\cos \phi_1 + j \sin \phi_1]} \quad (6)$$

$$x + jy = \frac{\theta_o(1 + g_1 \cos \phi_1 + g_1 \sin \phi_1) + \theta_1 g_1 \cos \phi_1 (1 + g_1 \sin \phi_1)}{1 + g_1^2 + 2g_1 \cos \phi_1} + j \frac{\theta_1 g_1 \sin \phi_1 (1 + g_1 \sin \phi_1 + g_1 \cos \phi_1)}{1 + g_1^2 + 2g_1 \cos \phi_1} \quad (7)$$

By equating the real and the imaginary parts of equation (7) in the two hand sides, we get two equations in four unknowns ($\theta_o, \theta_1, g_1, \phi_1$) and this is only for measuring angle in one direction (azimuth or elevation). If we consider the two directions, we have four equations in six unknowns ($\theta_{oa}, \theta_{oe}, \theta_{1a}, \theta_{1e}, g_1, \phi_1$). These equations can't be solved by only one pulse but requires more than one pulse. Therefore the monopulse radar uses two pulses instead of one to solve this problem, which is not the base of work of monopulse radar. If two-pulses are used, we assume that θ_o, θ_1 , and g_1 are the same during the two pulse intervals and there is only a change in ϕ_1 during the first and the second pulses and these values are ϕ_{11} and ϕ_{12} (subscript (1,2) for ϕ_1 refer to the first and second pulse). The complex measured angle (θ_j) takes the following two formulas $x_1 + jy_1$ and $x_2 + jy_2$ which represent two points in the complex plane, similar to equation (5) we can represents them as,

$$x_1 + jy_1 = \frac{\theta_o + \theta_1 g_1 e^{j\phi_{11}}}{1 + g_1 e^{j\phi_{11}}} \quad (8)$$

$$x_2 + jy_2 = \frac{\theta_o + \theta_1 g_1 e^{j\phi_{12}}}{1 + g_1 e^{j\phi_{12}}} \quad (9)$$

These two points determine a unique solution in the complex plane. Note that the center of the circle always lies on the real axis of the complex plane (the three points are enough to determine a unique circle in the complex plane), this circle determines an infinite number of θ_o, θ_1 and g_1 . For the solution to be unique, there is an additional consideration as follows, from equations (8) and (9), we have five unknown ($\theta_o, \theta_1, g_1, \phi_{11}, \phi_{12}$) in four equation. To have a unique solution we need one more equation, this equation can be obtained from the ratio of the sum channel during the first and the second pulse, which is expressed as

$$\left| \frac{S_2}{S_1} \right|^2 = \frac{1 + g_1^2 + 2g_1 \cos \phi_{12}}{1 + g_1^2 + 2g_1 \cos \phi_{11}} \quad (10)$$

Although this described method theoretically gives a solution based on only two pulses, some pairs of these pulses will give a good accuracy and others give poor, if

it happens that $\cos\phi_{11} = \cos\phi_{12}$, the solution is indeterminate. Therefore in practice as many pulses as possible should be used to have a good accuracy for this solution. In equation (2), if we consider $n=2$, the complex angle (θ_j) is written in the following form

$$\theta_j = \frac{\theta_o + \theta_1 g_1 e^{j\phi_1} + \theta_2 g_2 e^{j\phi_2}}{1 + g_1 e^{j\phi_1} + g_2 e^{j\phi_2}} \quad (11)$$

then as in equation (8), (9) we have two equations in seven unknowns ($\theta_o, \theta_1, \theta_2, g_1, g_2, \phi_1, \phi_2$), if we consider the two directions (azimuth and elevation), we have four equations in ten unknowns ($\theta_{oaz}, \theta_{oel}, \theta_{1az}, \theta_{1el}, \theta_{2az}, \theta_{2el}, g_1, g_2, \phi_1, \phi_2$). The measured complex angle (θ_j) can be written (as previous) in the form of $(x_1 + jy_1), (x_2 + jy_2), (x_3 + jy_3)$, and $(x_4 + jy_4)$ where the subscript 1,2,3,4 are referred to the four sequence pulses, These values represent eight equations in thirteen unknowns ($\theta_o, \theta_1, \theta_2, g_1, g_2, \phi_{11}, \phi_{12}, \phi_{13}, \phi_{14}, \phi_{21}, \phi_{22}, \phi_{23}, \phi_{24}$), the additional equations required to provide a unique solution are the ratios of the sum channels, as follows

$$\left| \frac{S_2}{S_1} \right|^2, \left| \frac{S_3}{S_2} \right|^2, \left| \frac{S_3}{S_1} \right|^2, \left| \frac{S_4}{S_3} \right|^2, \left| \frac{S_4}{S_2} \right|^2, \left| \frac{S_4}{S_1} \right|^2$$

For $n=3$, equation (3) can be written as follows

$$\theta_j = \frac{\theta_o + \theta_1 g_1 e^{j\phi_1} + \theta_2 g_2 e^{j\phi_2} + \theta_3 g_3 e^{j\phi_3}}{1 + g_1 e^{j\phi_1} + g_2 e^{j\phi_2} + g_3 e^{j\phi_3}} \quad (12)$$

if we consider six sequenced pulses, we have twenty five unknowns ($\theta_{0 \rightarrow 3}, g_{1 \rightarrow 3}, \phi_{11 \rightarrow 16}, \phi_{21 \rightarrow 26}, \phi_{31 \rightarrow 36}$), and the angle θ_j takes six complex values from $(x_1 + jy_1)$ to $(x_6 + jy_6)$, which makes twelve equations in addition to equations due to the ratio in sum channel

$$\left[\left(\left| \frac{S_6}{S_5} \right|^2 \text{ to } \left| \frac{S_6}{S_1} \right|^2 \right), \left(\left| \frac{S_5}{S_4} \right|^2 \text{ to } \left| \frac{S_5}{S_1} \right|^2 \right), \left(\left| \frac{S_4}{S_3} \right|^2 \text{ to } \left| \frac{S_4}{S_1} \right|^2 \right), \left(\left| \frac{S_3}{S_2} \right|^2 \text{ to } \left| \frac{S_3}{S_1} \right|^2 \right), \left(\left| \frac{S_2}{S_1} \right|^2 \right) \right]$$

that's make fifteen additional equations, so we have twenty five unknown in twenty seven equations, so it can be solved.

The conclusion of the above discussion is as follows, for N jamming signals, it's required $2N$ consequence pulses, and these pulses must satisfy that both $(\theta_1, \theta_2, \dots, \theta_N)$ and their relative amplitude ratios are constant during these pulses duration, which is so difficult to exist in practice because of the motion of the target will change these parameter during these pulses duration. Therefore we will consider $n=2$ in the jamming equation.

V. Conclusion

In the generated deceptive jamming signals, the change in the amplitude ratio makes large effect than the change in the phase difference on the real part of the complex measured error angle. The real value of the complex measured angle due to jamming with constant phase difference and different amplitude ratio has large variation at amplitude ratio less than three. This value converges to the value of the angle of the false target for higher amplitude ratio. There is no jamming effect at amplitude ratios less than one and for some values of phase difference. At these values, the measured angle equals to the angle of the real target. At least two jamming signals are required to have the complex error jamming angle to overcome the ECCM techniques that might be used by the target.

VI. References

- [1] George W. Ewell and Neal T. Alexander, **Principle of Modern Radar**, Artech house, Inc. 1997.
 - [2] Peyton Z. Peebles, JR., **Radar Principles**, John Wiley and Sons, Inc., 1998.
 - [3] Samuel M. Sherman " **Complex Indicated Angles Applied to Unresolved Radar Target and Multipath** ", IEEE Trans. on Aerospace and Electronic Systems, vol. AES-7, No. 1, January 1971.
 - [4] Peyton Z. Peebles, JR. and L. Goldman, JR. " **Radar Performance with Multipath Using the Complex Angle** ", IEEE Trans. on Aerospace and Electronic Systems, vol. AES-7, No. 1. January 1971.
-

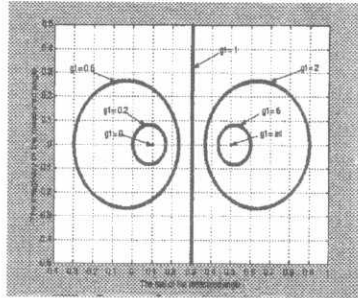


Fig.1. The complex measured angle for different amplitude ratio g_1

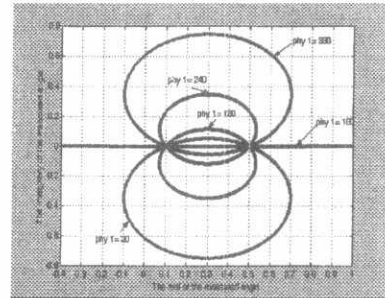


Fig.2. The complex measured angle for constant phase difference ϕ_1

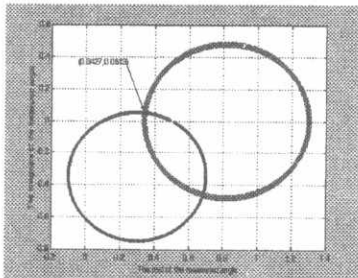


Fig.3. The complex measured angle at $g_1 = 1.5, \phi_1 = 30^\circ$

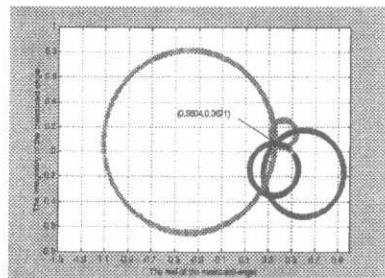


Fig.4. The complex measured angle at $g_1 = 1.5, g_2 = 2, \phi_1 = 30^\circ$, and $\phi_2 = 60^\circ$

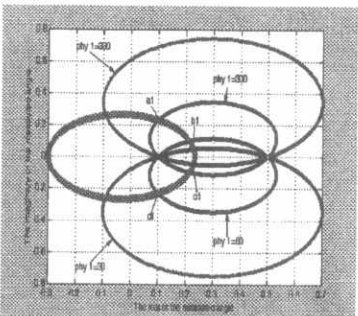


Fig.5. The complex measured angle at different phase difference ϕ_1 and constant amplitude ratio ($g_1 = 0.5$)

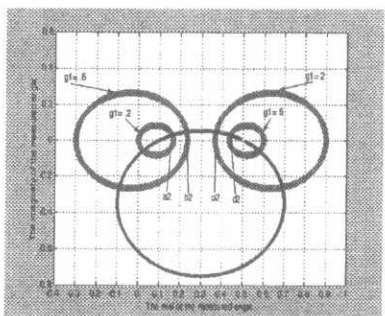


Fig.6. The complex measured angle for different amplitude ratio and constant phase difference ($\phi_1 = 30^\circ$)

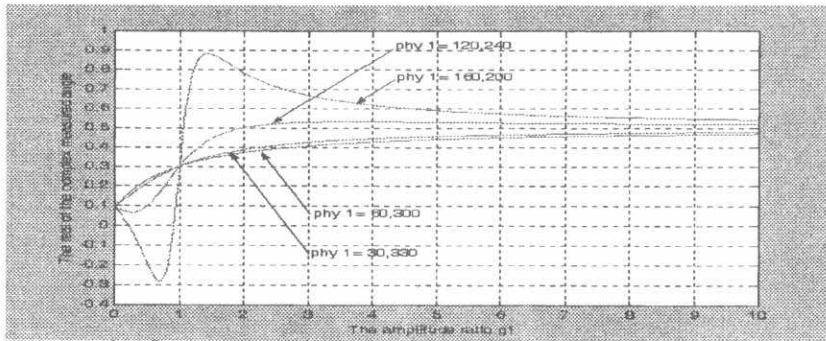


Fig.7. The complex measured angle versus amplitude ratio g_1

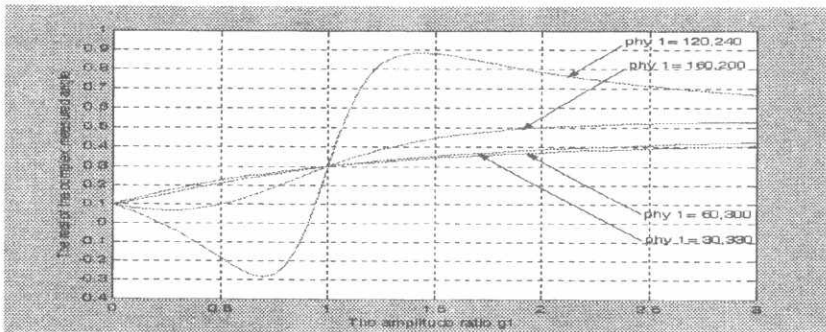


Fig.7a. zoom in on the complex measured angle versus amplitude ratio g_1

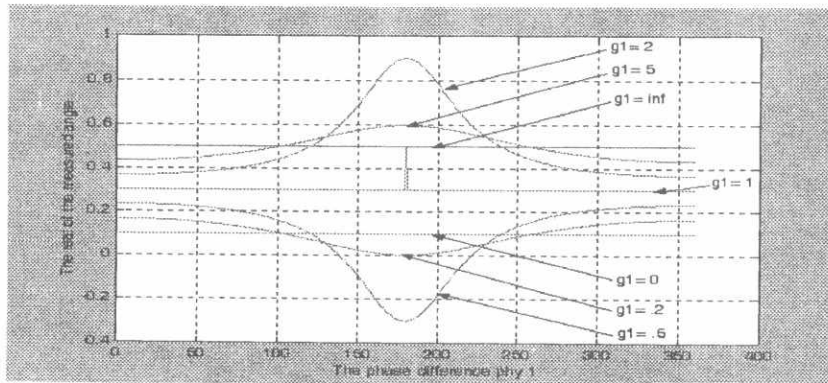


Fig.8. The real of the complex measured angle versus the phase difference for different amplitude ratio ϕ_1 .

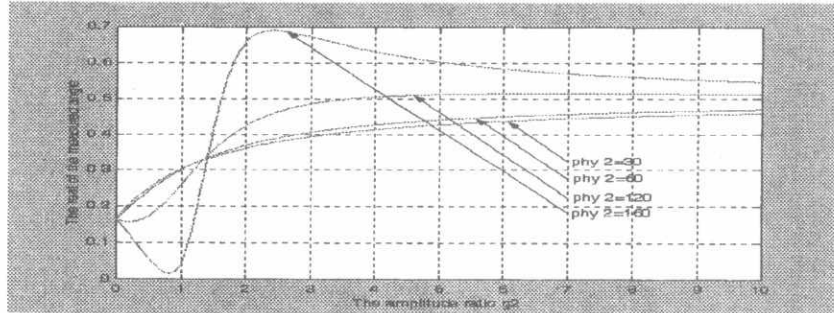


Fig.9. The real of the complex measured angle versus amplitude ratio g_2 at different constant phase ϕ_2 .

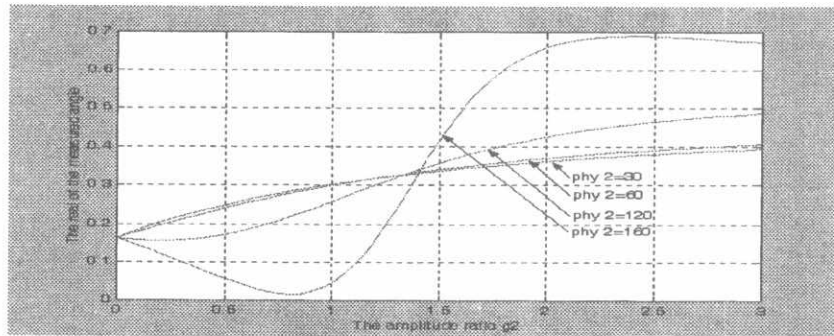


Fig.9a. zoom in on the real of the complex measured angle versus amplitude ratio g_2 at different constant phase ϕ_2 .

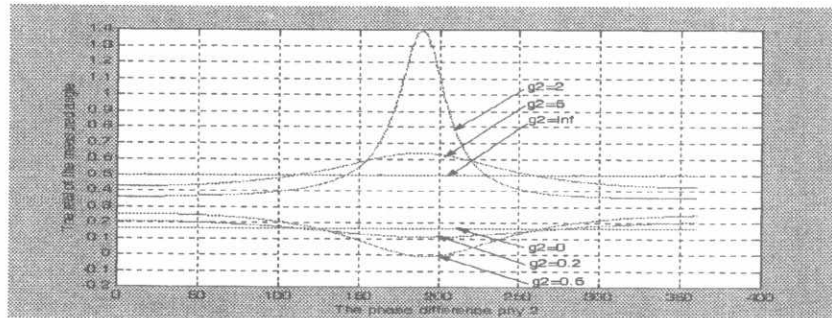


Fig.10. The real of the complex measured angle versus the phase difference ϕ_2 for different g_2 .